



# Spectroscopic Studies on the Interaction of Naphthyridines with DNA and Fluorescent Detection of DNA in Agarose Gel

G. Mahalakshmi<sup>1</sup> · B. Selvakumar<sup>2</sup> · K.N. Vennila<sup>1</sup> · P. Lakshmana Rao<sup>3</sup> · S. Madhuri<sup>3</sup> · M. Seenivasaperumal<sup>1</sup> · Kuppanagounder P. Elango<sup>1</sup> 

Received: 23 July 2020 / Accepted: 3 December 2020

© The Author(s), under exclusive licence to Springer Science+Business Media, LLC part of Springer Nature 2021

## Abstract

Four new naphthyridine derivatives (**R1–R4**) possessing amino acid or boronic acid moieties have been synthesized and characterized using <sup>1</sup>H and <sup>13</sup>C NMR, FT-IR, and mass spectral techniques. The mechanism of binding of these probes with calf thymus DNA (CT-DNA) has been delineated through UV-Vis, fluorescence, and circular dichroism (CD) spectral techniques along with thermodynamic and molecular docking studies. Small hypochromicity in absorption maximum of the probes without any shift in wavelength of absorption suggests groove binding mode of interaction of these probes with CT-DNA, confirmed by CD and <sup>1</sup>H NMR spectral data competitive binding assay with ethidium bromide (EB). CT-DNA quenches the fluorescence of these probes via a static quenching mechanism. In the case of **R1** and **R4**, the observed  $\Delta H^\circ < 0$  and  $\Delta S^\circ > 0$  suggest that these probes interact with CT-DNA through H-bonding and hydrophobic interactions, while in the interaction of **R2** and **R3**, van der Waals and H-bonding forces are found to be dominant ( $\Delta H^\circ < 0$  and  $\Delta S^\circ < 0$ ). Results of molecular docking investigations corroborate well with that of spectral studies, and these probes bind in the minor groove of DNA. These probes are found to be effective fluorescent staining agents for DNA in agarose gel in gel electrophoresis experiment with sensitivity comparable to that of EB, and DNA amounts as low as 37.5 ng are visually detectable in the gel.

**Keywords** DNA binding · DNA staining · Fluorescence · Naphthyridine · Electrophoresis

## Introduction

Deoxyribonucleic acid (DNA) is a critical natural molecule with interpretation and replication capacities and is the primary target for many biologically active compounds. Such bioactive compounds bind to DNA and help suppress or depress the replication and transcription processes. In recent years, a fair amount of work has been carried out on the binding interaction between bioactive molecules and DNA, as it provides information on the origin of diseases, structural properties of DNA, etc., and helps in designing newer chemotherapeutic

agents [1, 2]. In a wide variety of biological applications, detection and quantification of small amounts of DNA are extremely important. Over the years, various DNA visualization methods such as fluorescence, radiolabeling, organic dye, and silver staining have been reported, with each one has its advantage [3–9]. Among these methods, fluorescent staining of DNA is most common, particularly in gel electrophoresis. Ethidium bromide (EB), **I**, is the most widely used fluorescent probe for staining DNA once separated in gels. Though EB is used in gel electrophoresis to a larger extent, its handling and safe disposal require considerable attention as it is mutagenic and carcinogenic [10]. Therefore, to be used in the gel electrophoresis technique, the search for newer fluorescent probes for DNA staining is on and hence the present study. A literature review revealed that only very few fluorescent probes have been reported so far as DNA staining agents in gel electrophoresis, compared to voluminous work on small molecule-DNA interaction studies [11–13]. Very recently, we have reported the synthesis, DNA binding profile, and application of naphthyridine-2-carboxamides (**II**) as fluorescent DNA staining probes. We found that the sensitivity of **II**

✉ Kuppanagounder P. Elango  
drkpelango@rediffmail.com

<sup>1</sup> Department of Chemistry, Gandhigram Rural Institute, Deemed to be University, Gandhigram 624 302, India

<sup>2</sup> Anthem Biosciences Pvt. Ltd., Bangalore 560 099, India

<sup>3</sup> National Institute of Animal Biotechnology, Hyderabad 500 049, India

is comparable with that of EB, and DNA amounts as low as four nanograms are visually detectable in agarose gel [14].

In continuation of this, here in this work, we report four new amino/boronic acid appended naphthyridines as fluorescent probes for staining DNA in gel electrophoresis. Amino acid and boronic acid moieties were preferred as they possess pharmaceutical significance and would provide additional binding sites [15–20]. Studies on the mechanism of binding of these staining agents with DNA is a starting point for rational designing of newer agents with required properties. Hence, in the present study, the mechanism of interaction of the chosen naphthyridine derivatives with CT-DNA has been investigated using various spectral techniques and molecular docking studies. The main objectives, therefore, of the present endeavor are the synthesis, characterization, and DNA binding and staining studies of four new amino/boronic acid appended naphthyridines derivatives.

## Experimental

### Synthesis and Characterization of Probes (R1-R4)

**General Procedure for the Synthesis of 10-methoxydibenzo[b,h][1,6]naphthyridine-2-substituted Amino Acid Derivatives (R1 and R2)** The starting material 10-methoxydibenzo[b,h][1,6]naphthyridine-2-carboxylic acid (**1**) was prepared by adopting the procedure reported by us earlier [14]. To the stirred solution of **1** (200 mg) in DMF (1.0 mL, 5 v), corresponding amino acid ester (1.05 eq.) was added, and the reaction mass was cooled to 0–5 °C. Then HATU (1.15 eq) was added to the above reaction mass followed by triethylamine (3.0 eq.) at 0–5 °C, and the reaction mass was stirred for 1 h. After completion of the reaction (by TLC), the reaction mass was quenched with 5.0 mL of water and stirred for 10 min, filtered and washed with water. The resultant wet solid was treated with NaOH (2.0 eq.) in water (5.0 mL), and after completion of the reaction (by TLC), the pH was adjusted to 2–3 by adding HCl to get a light yellow product (Scheme 1).

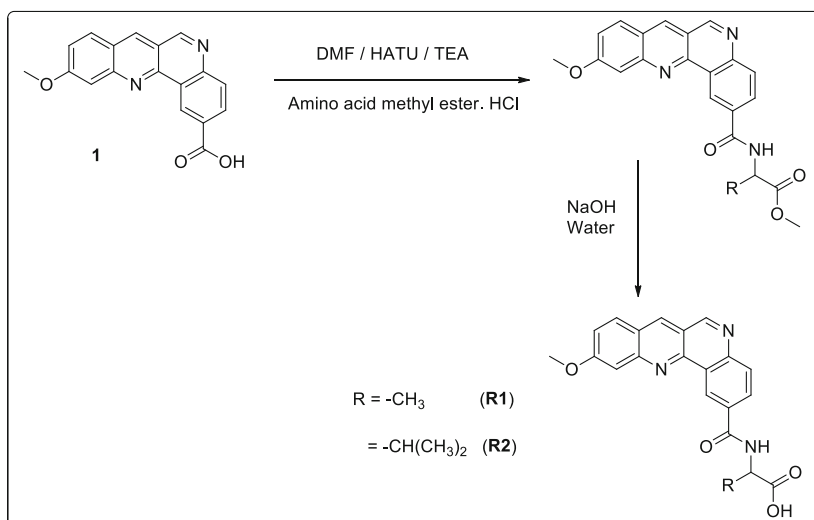
The probes **R1** and **R2** have been characterized using NMR, FT-IR, and mass spectral techniques and the results are:

**Probe R1.** Yield: 78%; m.p.: 250–254 °C; <sup>1</sup>H NMR (400 MHz, DMSO-d<sub>6</sub>, δ ppm): 1.47–1.49 (d, 3H, *J* = 7.6 Hz), 4.05–4.06 (d, 3H), 4.48–4.55 (m, 1H), 7.44–7.47 (m, 1H), 7.733–7.739 (d, 1H, *J* = 11.6 Hz, aromatic H), 8.18–8.20 (d, 1H, *J* = 8.4 Hz, aromatic H), 8.26–8.28 (d, 1H, aromatic H), 8.33–8.36 (m, 1H, aromatic H), 9.10–9.11 (d, 1H, *J* = 7.2 Hz, aromatic H), 9.29 (s, 1H, aromatic H), 9.55 (s, 1H, aromatic H), 9.70 (s, 1H, aromatic H) (Fig. S1); <sup>13</sup>C NMR (300 MHz, DMSO-d<sub>6</sub>, δ ppm): 17.0 (CH<sub>3</sub>), 48.5.3 (C-NH), 55.9 (OCH<sub>3</sub>), 106.1

(aromatic C), 118.2 (aromatic C), 121.2 (aromatic C), 122.8 (aromatic C), 123.5 (aromatic C), 124.1 (aromatic C), 130.6 (aromatic C), 132.7 (aromatic C), 138.0 (aromatic C), 147.1 (aromatic C), 147.3 (aromatic C), 151.8 (aromatic C), 155.9 (aromatic C), 162.9 (aromatic C), 165.9 (CONH) 174.3 (COOH) (Fig. S2); FT-IR (KBr, ν cm<sup>-1</sup>): 3416, 3267, 2967, 1619, 1595, 1416, 1233, 1168, 971, 698 (Fig. S3); LCMS (ESI) m/z found for C<sub>22</sub>H<sub>21</sub>N<sub>3</sub>O<sub>2</sub>[M + H]<sup>+</sup>: 375.6 (Fig. S4).

**Probe R2.** Yield: 65%; m.p.: 225–228 °C; <sup>1</sup>H NMR (400 MHz, DMSO-d<sub>6</sub>, δ ppm): 0.93–0.97 (d, 6H, 2 CH<sub>3</sub>'s), 1.66–1.70 (m, 1H), 1.774–1.779 (d, 1H), 1.85–1.90 (m, 1H), 4.07 (s, 3H, OCH<sub>3</sub>), 4.56–4.60 (m, 1H), 7.46–7.49 (m, 1H, aromatic H), 7.74–7.76 (d, 1H, *J* = 2.4 Hz, aromatic H), 8.23–8.25 (d, 1H, aromatic H), 8.28–8.31 (d, 1H, aromatic H), 8.38–8.40 (m, 1H, aromatic H), 9.09–9.11 (d, 1H, *J* = 7.6 Hz, aromatic H), 9.36 (s, 1H, aromatic H), 9.67 (s, 1H, aromatic H), 9.71–9.72 (d, 1H, aromatic H) (Fig. S5); <sup>13</sup>C NMR (300 MHz, DMSO-d<sub>6</sub>, δ ppm) δ: 21.2 (CH<sub>3</sub>), 23.0 (CH<sub>2</sub>), 24.6 (CH), 51.2 (C-NH), 56.1 (OCH<sub>3</sub>), 105.9 (aromatic C), 117.6 (aromatic C), 121.8 (aromatic C), 122.9 (aromatic C), 123.9 (aromatic C), 124.2 (aromatic C), 127.0 (aromatic C), 129.8 (aromatic C), 131.1 (aromatic C), 133.3 (aromatic C), 140.0 (aromatic C), 144.2 (aromatic C), 147.0 (aromatic C), 152.3 (aromatic C), 155.4 (aromatic C), 163.94 (aromatic C), 166.09 (CONH), 174.3 (COOH) (Fig. S6); FT-IR (KBr, ν cm<sup>-1</sup>): 3287, 2957, 1723, 1640, 1597, 1416, 1233, 1172, 848, 698 (Fig. S7); LCMS (ESI) m/z found for C<sub>22</sub>H<sub>21</sub>N<sub>3</sub>O<sub>2</sub>[M + H]<sup>+</sup>: 418.3 (Fig. S8).

**General Procedure for the Synthesis of 10-methoxydibenzo[b,h][1,6]naphthyridine-2-substituted Boronic Acid Derivatives (R3 and R4)** To the stirred solution of **1** (200 mg) in DMF (1.0 mL, 5 v) (R)-boro(alanine)-(+)-pinanedioltrifluoroacetate or (R)-boro(Leucine)-(+)-pinanedioltrifluoroacetate (1.05 eq.) was added and the reaction mass was cooled to 0–5 °C. Then HATU (1.15 eq.) was added to the above reaction mass followed by triethylamine (3.0 eq.) at 0–5 °C, and the reaction mass was stirred for 1 h. After completion of the reaction (by TLC), the reaction mass was quenched with 5.0 mL of water and stirred for 10 min, filtered and washed with water. The wet solid obtained was treated with 2 N HCl (5.0 mL) in methanol (5.0 mL) at ambient temperature and stirred for 2 h; upon completion of the reaction (by TLC), the reaction mass was washed with n-heptane (5.0 mL) and extracted with DCM (2 × 10.0 mL). Then DCM was dried over anhydrous sodium sulfate, and the concentration of the organic layer completely yielded the product as yellow solid (Scheme 2).

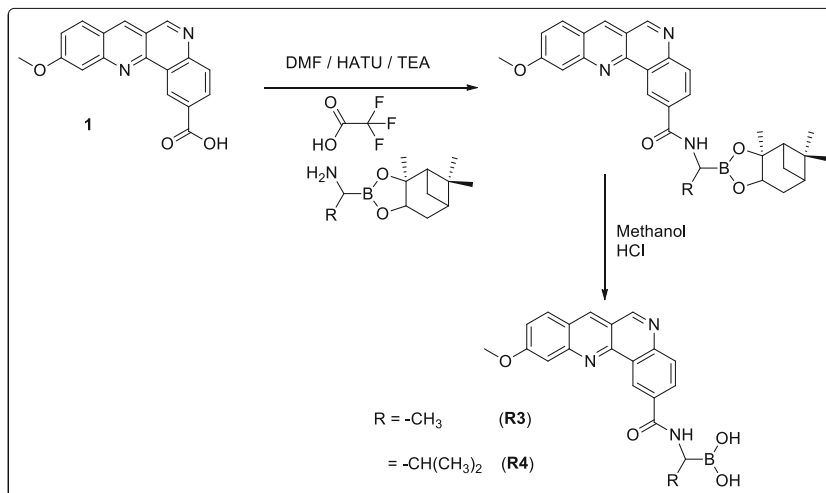
**Scheme 1** Synthesis of probes **R1** and **R2**

The probes **R3** and **R4** have been characterized using NMR, FT-IR, and mass spectral techniques and the results are:

**Probe R3.** Yield:24%; m.p.: 216–218 °C; <sup>1</sup>H NMR (400 MHz, DMSO-d<sub>6</sub>, δ ppm)1.20–1.24 (M, 3H, CH<sub>3</sub>), 4.05–4.07 (d, 3H, OCH<sub>3</sub>),7.43–7.47 (m, 1H, aromatic H), 7.69–7.74 (d, 1H, *J* = 16.4 Hz, aromatic H) 8.24–8.32 (m, 2H, aromatic H), 8.48–8.51 (m, 1H, aromatic H), 9.30–9.33(s, 1H aromatic H), 9.54 (s, 1H, aromatic H), 9.65–9.67 (d, 1H, aromatic H), 9.75–9.80(m, 2H, aromatic) (Fig. S9); <sup>13</sup>C NMR (300 MHz, DMSO-d<sub>6</sub>, δ ppm) 15.8(CH<sub>3</sub>), 56.1 (OCH<sub>3</sub>), 105.6 (aromatic C), 117.1 (aromatic C), 121.6 (aromatic C), 122.5 (aromatic C), 123.05(aromatic C), 124.10 (aromatic C), 127.8(aromatic C), 129.8 (aromatic C), 130.7 (aromatic C), 139.46 (aromatic C), 145.7 (aromatic C), 151.9 (aromatic C), 156.59 (aromatic C), 163.70 (aromatic C), 169.8 (CONH) (Fig. S10); FT-IR (KBr, ν cm<sup>-1</sup>): 3401, 2967,1608, 1477,1414, 1235, 1172, 848, 697 (Fig. S11); LCMS

(ESI) *m/z* found for C<sub>22</sub>H<sub>21</sub>N<sub>3</sub>O<sub>2</sub>[M + H]<sup>+</sup>: 376.2 (Fig. S12).

**Probe R4:** Yield: 20%; m.p.: 210–215 °C;<sup>1</sup>H NMR (400 MHz, DMSO-d<sub>6</sub>, δ ppm) 0.94–0.99 (d, 6H, *J* = 6.8 Hz, 2 CH<sub>3</sub>'s), 1.529–1.547(d,2H), 1.63–1.72(m,1H), 4.06 (s, 3H, OCH<sub>3</sub>),7.44–7.46 (m, 1H, aromatic H), 7.721–7.727 (d, 1H, *J* = 2.4 Hz, aromatic H), 7.94(s, 1H aromatic H), 8.16–8.18(d, 1H, aromatic H), 8.27–8.31 (m, 2H, aromatic H), 8.84–8.86 (m, 1H, aromatic H),9.27 (s, 1H aromatic H), 9.54 (s, 1H, aromatic H), 9.65–9.66 (d, 1H, aromatic H) (Fig. S13); <sup>13</sup>C NMR (300 MHz, DMSO-d<sub>6</sub>, δ ppm)11.0 (CH<sub>3</sub>),15.0(CH<sub>2</sub>),25(CH), 56.1 (OCH<sub>3</sub>), 106.0 (aromatic C), 117.8 (aromatic C), 121.7 (aromatic C), 122.9 (aromatic C), 124.1 (aromatic C), 127.5(aromatic C), 129.83 (aromatic C), 131.0 (aromatic C), 132.9(aromatic C), 133.3(aromatic C),139.5 (aromatic C), 147.0 (aromatic C), 152.1 (aromatic C), 155.6

**Scheme 2** Synthesis of probes **R3** and **R4**

(aromatic C), 163.9 (aromatic C), 166.6 (CONH) 174.1 (C-B) (Fig. S14); FT-IR (KBr,  $\nu$   $\text{cm}^{-1}$ ): 3298, 2950, 1628, 1526, 1416, 1230, 1164, 851, 767 (Fig. S15); LCMS (ESI)  $m/z$  found for  $\text{C}_{22}\text{H}_{21}\text{N}_3\text{O}_2[\text{M} + \text{H}]^+$ : 418.3 (Fig. S16).

## Results and Discussion

The following four new amino acid or boronic acid appended naphthyridine derivatives were synthesized and characterized using NMR, FT-IR, and mass spectral techniques.

The binding behavior of these probes with calf thymus DNA (CT-DNA) has been investigated using UV-Vis, fluorescence, and circular dichroism spectral studies. Thermodynamic parameters have been determined to delineate the nature of the attraction forces between the probes and CT-DNA. Molecular docking studies have also been carried out to substantiate the results of spectral analyses. To demonstrate the applicability of these probes, DNA staining studies were carried out in agarose gel using plasmid DNA.

### UV-Vis Spectral Studies

UV-Vis spectroscopy is one of the most effective methods of investigating the interaction of small molecules with DNA. The probes' UV-Vis spectra have been recorded in HEPES buffer/DMSO (pH 7.4) medium. As seen in Figs. 1 and S17–S19, free probes exhibited two absorption bands: a strong one

around 285 nm corresponds to the  $\pi$ - $\pi^*$  transition and the other around 385 nm due to  $n$ - $\pi^*$  transition. It is evident from these figures that upon adding increasing amounts of CT-DNA to the solution of these probes, the intensity of these two bands experienced a very slight decrease (hypochromicity) without any significant shift in wavelength of absorption maximum. Such an electronic spectral change suggested that these probes bind to CT-DNA, preferably through a non-intercalative mode of binding [21].

### Fluorescence Spectral Studies

All the four probes (R1–R4), when excited at  $\lambda_{\text{ex}}$  250 nm, give strong emission around 450 nm in HEPES buffer/DMSO (pH 7.4) medium (Fig. 2 and S20–S30). Upon adding increasing amounts of CT-DNA to these probes, the fluorescence of the probes gets quenched with no apparent shift in the wavelength of emission maximum. Such a fluorescence quenching indicated that these probes interact with CT-DNA. The quenching mechanism was established by analyzing the fluorescence data using the Stern-Volmer equation [22, 23].

$$F_0/F = 1 + K_{\text{SV}}[Q] \quad (1)$$

Where  $F_0$  and  $F$  are the probes' fluorescence intensities in the absence and presence of the CT-DNA, respectively,  $K_{\text{SV}}$  is the Stern-Volmer quenching constant, which was determined from the linear plots of  $F_0/F$  versus  $[Q]$  (Fig. 3 and S31–S33) at three different temperatures. As seen from the data collected in Table 1,  $K_{\text{SV}}$  values were found to decrease with an

**Fig. 1** UV-Vis spectra of R1 [100  $\mu\text{M}$ ] with incremental addition of CT-DNA [0–47 nM] in HEPES buffer/DMSO (pH 7.4) medium

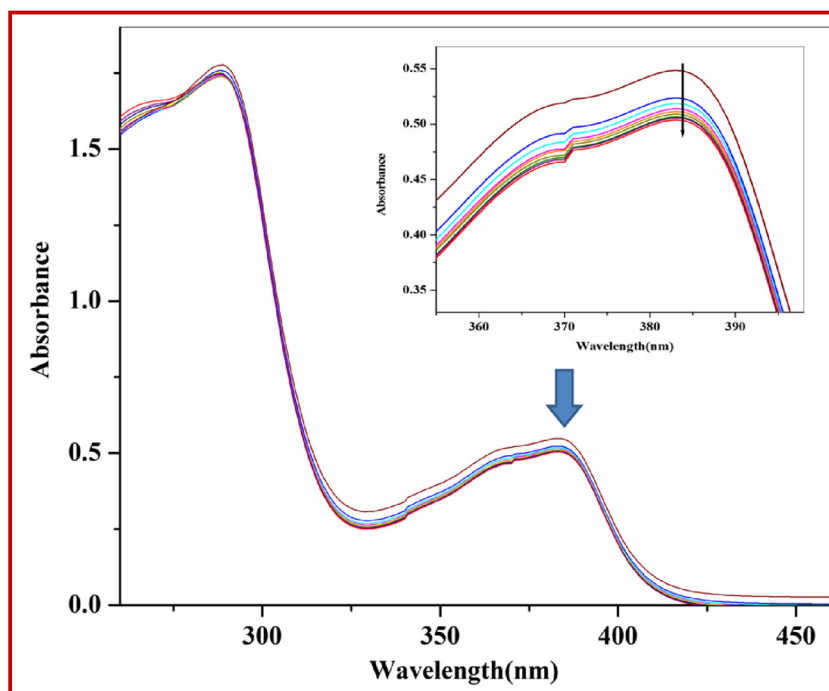
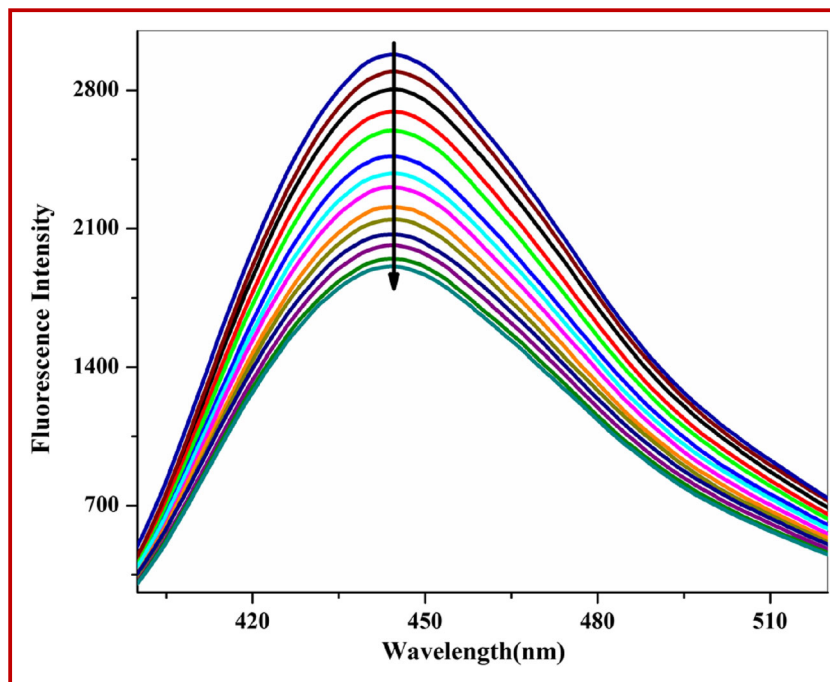


**Fig. 2** Fluorescence spectra of **R1** [25  $\mu$ M] in HEPES buffer/ DMSO medium (pH 7.4) upon addition of CT-DNA [0–325 nM] at 298 K



increase in temperature, suggesting that CT-DNA quenched these probes' fluorescence via a static quenching mechanism [24, 25].

**Thermodynamic Analysis**

The nature of the binding forces that hold small molecules with DNA in their complexes can be identified using thermodynamic parameters such as enthalpy change ( $\Delta H^\circ$ ), entropy change ( $\Delta S^\circ$ ), and free energy change

( $\Delta G^\circ$ ). These thermodynamic parameters can be calculated from the temperature-dependent binding constants for the interaction of small molecules with DNA. In the present study, the binding constants ( $K_b$ ) for the interaction of the probes **R1–R4** with CT-DNA have been determined from the fluorescence data using the following equation at three different temperatures [26, 27].

$$\log(F_0 - F/F) = \log K_b + n \log [Q] \tag{2}$$

**Fig. 3** Stern-Volmer plots for quenching of fluorescence of **R1** by CT-DNA at three different temperatures

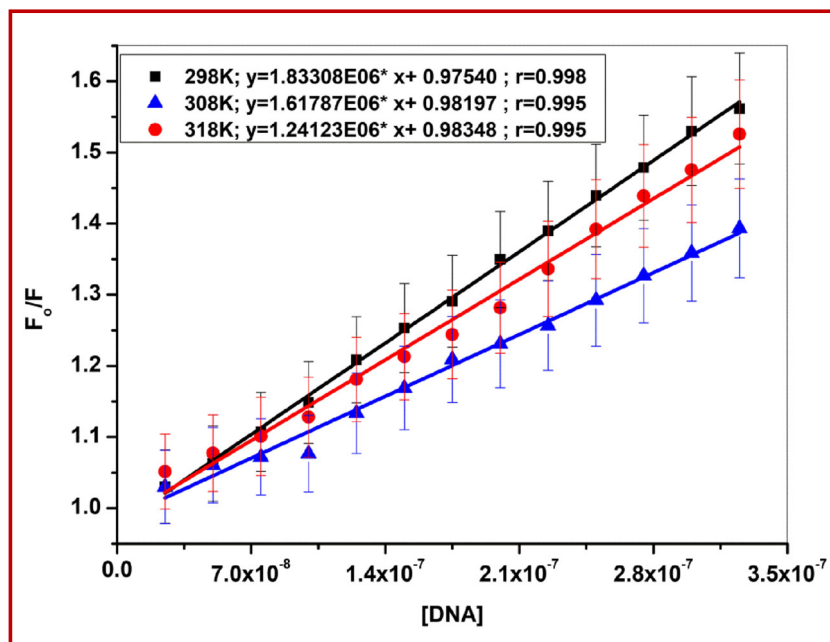


**Table 1** Stern-Volmer constants ( $K_{SV}$ ), binding constants ( $K_b$ ) and the related thermodynamic parameters for the interaction of the probes **R1–R4** with CT-DNA

Probe	Temp. (K)	$K_{SV}$ ( $M^{-1}$ )	$K_b$ ( $M^{-1}$ )	$\Delta H^\circ$ $\text{kJK}^{-1} \text{mol}^{-1}$	$\Delta S$ $\text{JK}^{-1} \text{mol}^{-1}$	$\Delta G^\circ$ $\text{kJK}^{-1} \text{mol}^{-1}$
R1	298	$1.8 \times 10^6$	$11 \times 10^6$	0.03	38	-40
	308	$1.6 \times 10^6$	$6.6 \times 10^6$			
	318	$1.2 \times 10^6$	$5.3 \times 10^6$			
R2	298	$1.4 \times 10^6$	$5.5 \times 10^6$	-0.09	-165	-38
	308	$1.0 \times 10^6$	$2.0 \times 10^6$			
	318	$0.95 \times 10^6$	$0.59 \times 10^6$			
R3	298	$2.5 \times 10^6$	$1.0 \times 10^8$	-0.02	-408	-46
	308	$1.9 \times 10^6$	$1.7 \times 10^7$			
	318	$1.5 \times 10^6$	$1.4 \times 10^6$			
R4	298	$3.6 \times 10^6$	$12 \times 10^5$	-0.03	3.1	-35
	308	$3.3 \times 10^6$	$7.5 \times 10^5$			
	318	$3.1 \times 10^6$	$5.1 \times 10^5$			

Where  $F_0$  and  $F$  are the fluorescence intensities of the probes in the absence and presence of the quencher, CT-DNA, respectively, and  $K_b$  is the binding constant. The binding constant values were computed from the linear plots of  $\log(F_0 - F)/F$  versus  $\log[Q]$  (Fig. 4 and S34–S36). The  $K_b$  values, thus obtained, are also summarized in Table 1. The order of these probes'  $K_b$  values for the interaction with CT-DNA is observed to be **R3** > **R1** > **R2** > **R4**. Among the probes under investigation, the one naphthyridines derivative possessing boronic acid moiety with relatively less steric hindrance (**R3**) binds strongly with the CT-DNA. The binding of **R3** with CT-DNA is much stronger than that of naphthyridine-2-carboxamides reported by us [14], and many cyanine-styryl dyes [28, 29] and cyanine dyes [30] reported earlier. Thus, as spelled in the introduction

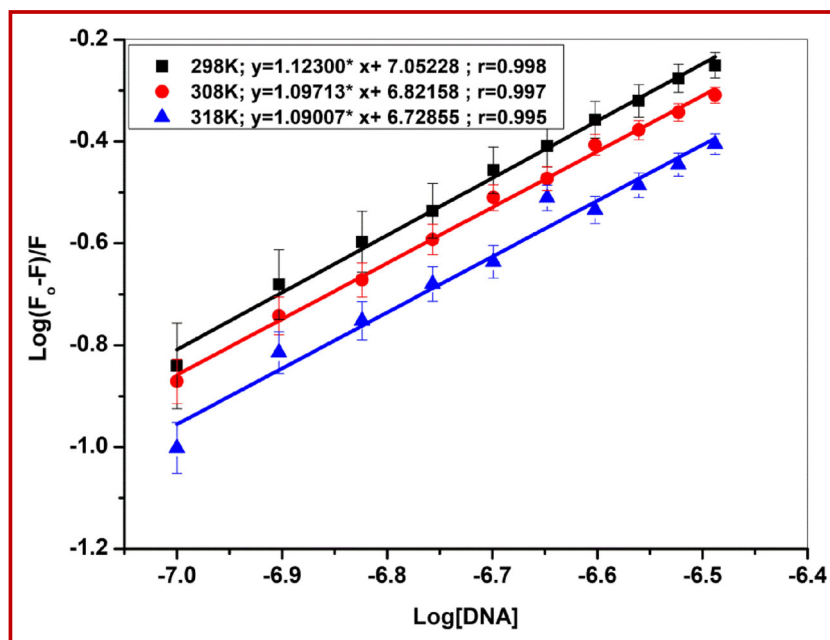
section, the introduction of boronic acid moiety substantially enhanced naphthyridine derivatives' binding ability. With an increase in temperature, the  $K_b$  values' trends are following that of the  $K_{SV}$  values.

From these  $K_b$  values, the thermodynamic parameters were calculated using van't Hoff and Gibbs-Helmholtz equations [31]:

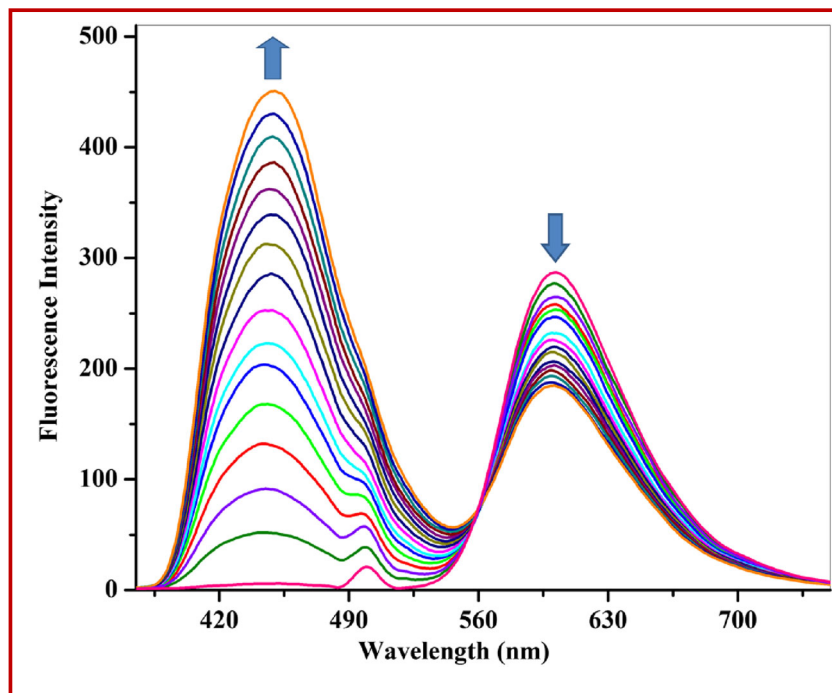
$$\log K_b = \log(\Delta H/2.303RT) + (\Delta S/2.303R) \quad (3)$$

$$\Delta G_0 = \Delta H_0 - T\Delta S_0 \quad (4)$$

In the present study, plots of  $\log K_b$  versus  $1/T$  (Fig. S37–S40) were found to be linear, and the enthalpy ( $\Delta H^\circ$ ) and entropy ( $\Delta S^\circ$ ) changes were obtained from the slope and intercept, respectively, of the linear plots. The thermodynamic parameters for the interaction of the probes with CT-DNA are

**Fig. 4** Plot of  $\log(F_0 - F)/F$  versus  $\log[Q]$  for interaction of **R1** with CT-DNA at three different temperatures

**Fig. 5** Fluorescence changes for the titration of **R1** [0–15  $\mu\text{M}$ ] with EB/CT-DNA complex



also given in Table 1. It is evident from the data that in all the cases, the free energy change ( $\Delta G^\circ$ ) was found to be negative, indicating that the binding of the probes with CT-DNA is a spontaneous process. Further, in the case of **R1** and **R4**, the values of enthalpy and entropy changes ( $\Delta H^\circ < 0$  or  $\Delta H^\circ \approx 0$  and  $\Delta S^\circ > 0$ ) were found to be negative and positive, respectively. Wang et al. reported that  $\Delta H^\circ < 0$  and  $\Delta S^\circ > 0$  could be recognized due to H-bonding and hydrophobic

interactions, respectively [32]. While in the case of **R2** and **R3**, the observed  $\Delta H^\circ < 0$  or  $\Delta H^\circ \approx 0$  and  $\Delta S^\circ < 0$  suggested that these probes bind with CT-DNA via van der Waals and H-bonding forces [33]. Therefore, in the present study, the binding of these probes with CT-DNA might be driven by H-bonding and hydrophobic interactions along with van der Waals forces. Parallel observations were made by Tian et al. during the study on the interaction between naphthalimide-

**Fig. 6** Circular dichroism spectra of CT-DNA in the presence of probes **R1-R4** in HEPES buffer/DMSO (pH 7.4) medium

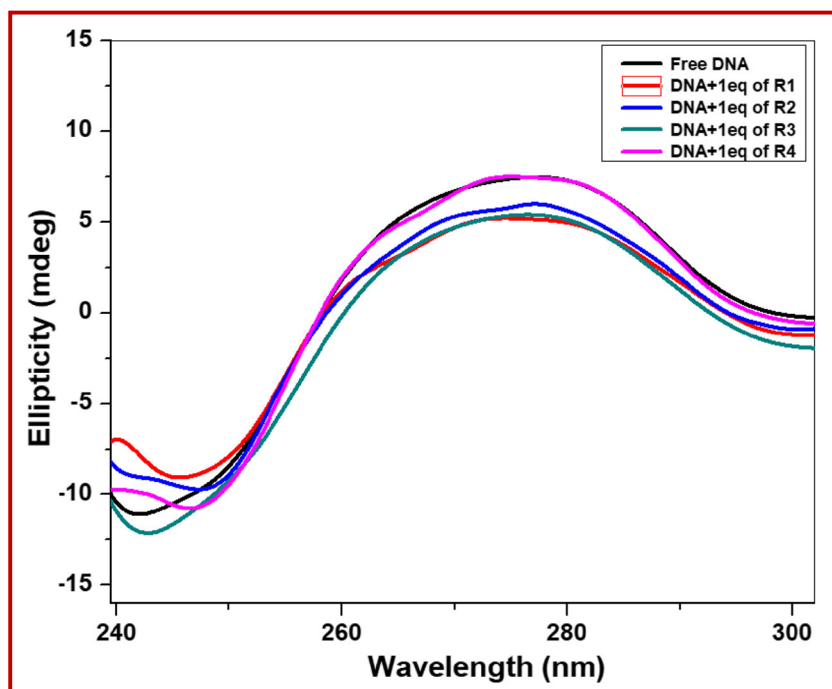
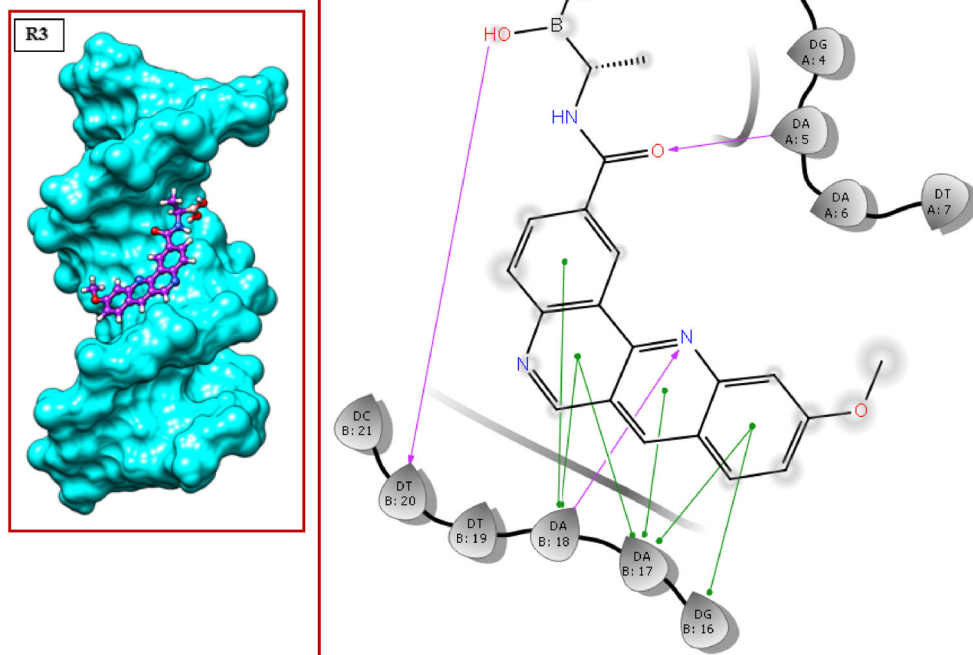


**Fig. 7** Docking results showing H-bonding and  $\pi$ - $\pi$  interactions of **R3** with residues of DNA



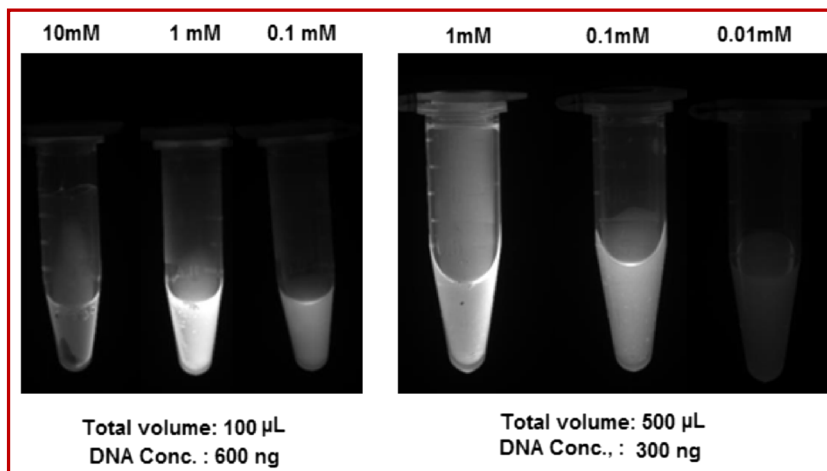
polyamine conjugates and herring sperm DNA. These structurally similar conjugates exhibited a different variety of enthalpy and entropy changes [34].

### Competitive Binding Assay

The mode of binding of small molecules with DNA is commonly determined using ethidium bromide (EB) as the fluorophore probe, as the EB-DNA complex emits strongly. It is well recognized that EB binds to the base pairs of DNA through intercalation mode. Any molecule that competes with DNA via a similar intercalative mode would displace EB from the EB-DNA complex and consequently decrease its

fluorescence to a more considerable extent. Therefore, a competitive binding assay has been carried out by adding increasing amounts of these probes **R1-R4** to the solution of the EB/CT-DNA complex. As seen in Figs. 5 and S41–S43, EB/CT-DNA complex emits at 601 nm when excited at 250 nm. On adding increasing amounts of **R1-R4** to this complex, the intensity of emission at 601 nm decreased to a lesser extent suggesting that these probes bind to CT-DNA through a non-intercalative mode of binding [35, 36]. At the same time, with the addition of increasing amounts of these probes to the EB/CT-DNA complex, the intensity of emission around 450 nm, corresponding to the free probe, increased significantly, suggesting that these probes remains mostly free (or loosely

**Fig. 8** DNA staining at different concentrations of **R3**



bound to CT-DNA) and doesn't intercalate with the base pairs of CT-DNA by dislodging EB. Thus, these probes might bind in the groove of the CT-DNA molecule.

### <sup>1</sup>H NMR Spectral Study

A <sup>1</sup>H NMR spectral study on the binding of these probes with CT-DNA was also carried out to validate spectroscopic studies' results. In this attempt, guanosine nucleoside was used as a model for DNA. The <sup>1</sup>H NMR spectra of guanosine were recorded in the absence and presence of these probes in DMSO-d<sub>6</sub> [14, 37]. <sup>1</sup>H NMR spectrum of free guanosine showed signals at 6.461, 7.939, and 10.633 ppm due to –NH<sub>2</sub>, imidazole C-H and –NH protons, respectively (Fig. S44). As seen in figs. S45–S48, on adding one equivalent of **R1–R4** individually to the solution of guanosine, the signals corresponding to all these protons exhibited shifts indicating an interaction of these probes with CT-DNA. Particularly the strong signal due to –NH proton has presented a noticeable downfield shift. The probe **R3** has brought the maximum downfield shift in the –NH proton with a  $\Delta\delta$  value of 1.065 ppm, and the probe **R4** has fetched the minimum shift in the signal ( $\Delta\delta$  0.016 ppm). The magnitude of the  $\Delta\delta$  values corroborates well the trend binding constant values of the probe/CT-DNA complexes determined using fluorescence titration data. That is, probe **R3** with a relatively higher binding constant value showed the more considerable  $\Delta\delta$  value. These observations suggested that these probes interact with CT-DNA through H-bonding, possibly using N-H protons of the guanosine nucleoside.

### Circular Dichroism Spectral Studies

As circular dichroism spectral studies possess high sensitivity and accuracy, it is frequently used to investigate the conformational changes of DNA upon binding with small molecules. The CD spectra of CT-DNA recorded in the absence and presence of these probes **R1–R4** are depicted in Fig. 6. Free CT-DNA exhibited a negative band at 245 nm corresponding to right-handed helicity and a positive band at 277 nm due to base stacking, which was the characteristic CD spectra of B-conformation of DNA. With the addition of one equivalent of these probes to the CT-DNA solution, the intensities of the two bands showed only a very marginal shift, suggesting that these probes interact with CT-DNA through groove binding mode. It is well known that the groove binding of small molecules doesn't bring massive structural/conformational changes in DNA [38, 39] (Fig. 7).

### Molecular Docking Studies

Molecular docking studies have been carried out to clarify further the mode of binding of these probes with DNA.

Here, the molecular docking of these probes (keeping them flexible) and the rigid DNA (PDB id: 1BNA) was carried out, and the modeling results are illustrated in Figures 7 and S49–S51. As seen in the figure, in the energetically most favorable conformation, the probes docked into the minor groove of DNA, and the probes interact with DNA through H-bonding and hydrophobic interactions, which is in good agreement with the results of thermodynamic studies. Further, the probe **R3** binds strongly in the A-T base pair with a relatively larger combination of H-bonding, hydrophobic, and  $\pi$ - $\pi$  stacking interactions. The free energy changes ( $\Delta G$ ) for the binding of these probes with DNA were computed to be –4.58, –4.68, –4.52, and –4.71 kcal mol<sup>–1</sup>, for **R1**, **R2**, **R3**, and **R4**,

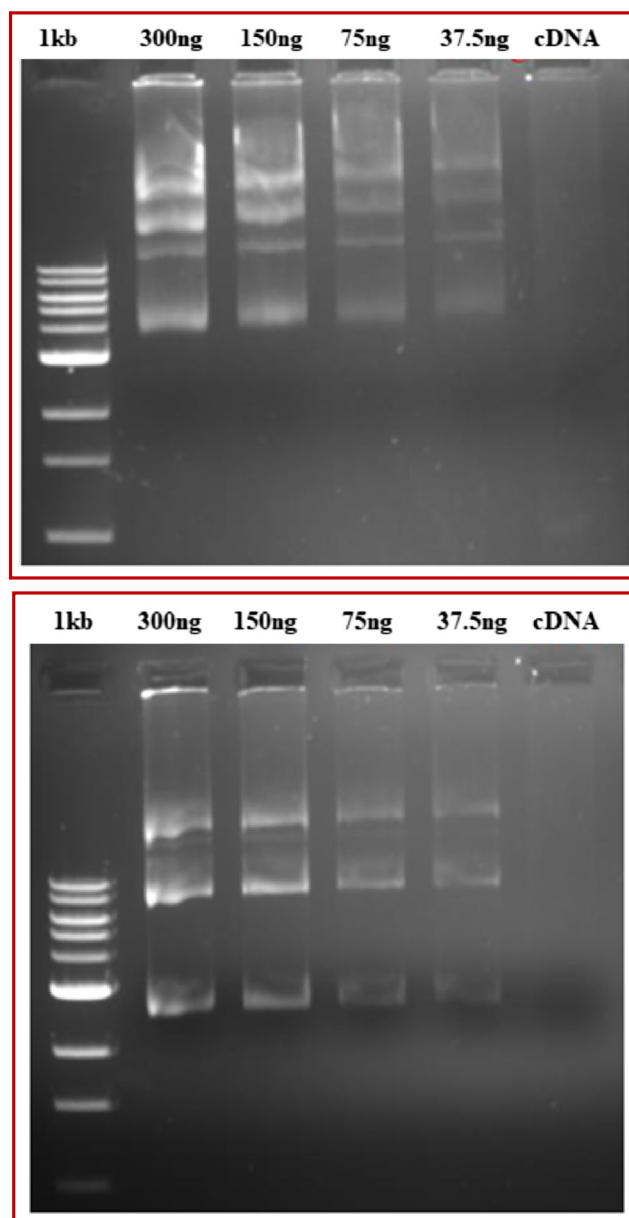


**Fig. 9** Staining of DNA fragments with **R3** (Top) and EB (Bottom) on a 1% agarose gel

respectively. These free energy change values are lower than the experimental value ( $-9.98$ ,  $-9.92$ ,  $-10.39$ , and  $-9.05$  kcal mol<sup>-1</sup>, respectively), and this mismatch could be due to the exclusion of solvent and/or rigidity of DNA molecule in the docking studies [40]. Furthermore, a competitive displacement docking was also performed using EB (Fig. S52). The results clearly showed that these probes bind to the minor groove of DNA while EB intercalates into DNA base pairs. Thus, it is evident from the combined results of spectroscopic, thermodynamic, and molecular docking studies that these probes bind with DNA in the minor groove, and the dominating interaction forces between them are H-bonding, van der Waals, and hydrophobic interactions.

### DNA Staining Studies

Fluorescent detection of DNA in gel electrophoresis experiments has been done to show these probes' practical application. Electrophoresis experiments were carried out using agarose gel, as reported by us earlier [14]. In a typical experiment, initially 1% agarose gel was prepared in 1X TAE with different concentrations (10, 1, 0.1, and 0.01 mM) of the test compounds to identify the minimal concentration of the test compound that gave fluorescence upon binding to a known concentration of DNA (600 ng in 100  $\mu$ L volume) (Fig. 8 and S53). Based on the results, 0.1 mM concentration of **R1** and **R3** and 1 mM concentration of **R2** and **R4** were taken for electrophoresis experiments. The gel was allowed to get solidified for 30–40 min at room temperature. Upon solidification, the gel was immersed in the tank containing 1X TAE buffer. Plasmid DNA (TOPO TA clone with an available insert construct cloned into it) samples were mixed in a 6:1 ratio with 6X DNA loading dye (New England Biolabs). The agarose gel was allowed to run at 100 V, 100 mA, and 10 W for 30–40 min and visualized under geldoc (Syngene G: Box model No. Chemi HR-1.4; Software: Genesys). The gel photographs, thus obtained, are depicted in Figs. 9 and S54–S56. As seen in the figures, all the probes, except **R4**, have performed on par with ethidium bromide (10 mg/ml) in the staining process. In all these cases, the least concentration of 37.5 ng of DNA could be visualized under UV light, while in probe **R4** staining, 37.5 ng of DNA was only faintly visualized. Further, the probes **R1** and **R3** were found to be more efficient at a concentration of 0.1 mM than the probe **R2**. The relatively better performance of the probes **R3** and **R1** may be due to their relatively higher binding ability with DNA, as evidenced from the preceding results of optical spectroscopic studies. Thus, these probes could well be used as fluorescent probes for DNA staining in agarose gel and are efficient and sensitive for DNA analysis comparable with that of the commonly used fluorescent staining agent, EB.

### Conclusion

To conclude, we have synthesized four new naphthyridine derivatives possessing amino acid or boronic acid and characterized those using FT-IR, NMR, and mass spectral techniques. UV-Vis, fluorescence, and circular dichroism (CD) spectral methods have been employed to investigate these probes' mode of binding with CT-DNA. These spectral studies' results, along with competitive binding with EB and <sup>1</sup>H NMR studies, revealed that these probes bind with CT-DNA through groove binding mode. Thermodynamic analysis indicated that the main forces operating in the probe-DNA binding are H-bonding, hydrophobic, and van der Waals forces, which is strongly supported by molecular docking studies. The boronic acid appended probe **R3** ( $K_b$  in the order of  $10^8$  M<sup>-1</sup> at 298 K) was found to bind with CT-DNA relatively stronger than its carboxamide derivatives ( $K_b$  in the order of  $10^6$  &  $10^7$  M<sup>-1</sup> at 298 K) reported earlier [14]. The applicability of these probes as effective fluorescent staining agents for DNA in agarose gel in gel electrophoresis experiment has also been demonstrated. The results showed that the sensitivity of staining is comparable with that of EB in agarose gel.

**Supplementary Information** The online version contains supplementary material available at <https://doi.org/10.1007/s10895-020-02658-0>.

**Availability of Data and Materials** Not applicable.

**Authors Contributions** G.Mahalakshmi: Investigation, Formal analysis and Writing; B.Selvakumar: Methodology; K.N.Vennila: Software and Analysis; P.Lakshmana Rao: Software and Analysis; S.Madhuri: Methodology, Software and Analysis; M.Seenivasaperumal: Software and Analysis; Kuppanagounder P. Elango: Conceptualization, Review, Supervision.

### Compliance with Ethical Standards

**Competing Interests** None

### References

1. Andaloussi M, Moreau E, Masurier N, Lacroix J, Gaudreault RC, Chezal JM, Laghdach AE, Canitrot D, Debiton E, Teulade JC, Chavignon O (2008) Novel imidazo[1,2-a]naphthyridinic systems (part 1): synthesis, antiproliferative and DNA-intercalating activities. *Eur J Med Chem* 43:2505–2517. <https://doi.org/10.1016/j.ejmech.2008.02.017>
2. Hawtin RE, Stockett DE, Byl JAW, McDowell RS, Tan N, Arkin MR, Conroy A, Yang W, Osheroff N, Fox JA (2010) Voreloxin is an anticancer quinolone derivative that intercalates DNA and poisons topoisomerase II. *PLoS One* 5:e10186. <https://doi.org/10.1371/journal.pone.0010186>
3. Kovalska VB, Volkova KD, Losytskyy MY, Tolmachev OI, Balanda AO, Yarmoluk SM (2006) 6,6-Disubstituted benzothiazole trimethine cyanines—new fluorescent dyes for DNA detection. *Spectrochim Acta A* 65:271–277. <https://doi.org/10.1016/j.saa.2005.10.042>

4. Erve A, Saoudi Y, Thiroit S, Landras CG, Florent JC, Nguyen CH, Grierson DS, Popov AV (2006) BENA435, a new cell-permeant photoactivated green fluorescent DNA probe. *Nucleic Acids Res* 34:1–13. <https://doi.org/10.1093/nar/gkl011>
5. Cong W, Chen M, Zhu Z, Liu Z, Nan J, Ye W, Ni M, Zhao T, Jin L (2013) A shortcut organic dye-based staining method for the detection of DNA both in agarose and polyacrylamide gel electrophoresis. *Analyst* 138:1187–1194. <https://doi.org/10.1039/C2AN36079A>
6. Sonmezoglu OA, Ozkay K (2015) A new organic dye-based staining for the detection of plant DNA in agarose gels. *Nucleos Nucleot Nucl* 34:515–522. <https://doi.org/10.1080/15257770.2015.1017581>
7. Schmidt F, Schmidt J, Riechers A, Haase S, Bosserhoff AK, Heilmann J, König B (2010) DNA staining in agarose gels with Zn<sup>2+</sup>-cyclen-pyrene. *Nucleos Nucleot Nucl* 29:748–759. <https://doi.org/10.1080/15257770.2010.515282>
8. Cong WT, He HZ, Zhu ZX, Ye CX, Yang XY, Cho JK, Jin LT, Li XK (2010) Improved conditions for silver-ammonia staining of DNA in polyacrylamide gel. *Electrophoresis* 31:1662–1665. <https://doi.org/10.1002/elps.200900786>
9. Chen M, Cong WT, Zhou X, Zhu ZX, Ye WJ, Ling J, Ni MW, Jin LT (2013) A method for sensitive staining of DNA in polyacrylamide gels using basic fuchsin. *Bioanalysis* 5:1545–1554. <https://doi.org/10.4155/bio.13.113>
10. Lunn G, Sansone EB (1987) Ethidium bromide: Distraction and decontamination of the solution. *Anal Biochem* 162:453–458. [https://doi.org/10.1016/0003-2697\(87\)90419-2](https://doi.org/10.1016/0003-2697(87)90419-2)
11. Okuma K, Koga T, Ozaki S, Suzuki Y, Horigami K, Nagahora N, Shioji K, Fukuda M, Deshimaru M (2014) One-pot synthesis of dibenzo[b,h][1,6]naphthyridines from 2-acetylaminobenzaldehyde: application to a fluorescent DNA-binding compound. *Chem Commun* 50:15525–15528. <https://doi.org/10.1039/c4cc07807a>
12. Okuma K, Oba A, Kuramoto R, Iwashita H, Nagahora N, Shioji K, Noguchi R, Fukuda M (2017) Synthesis and fluorescence properties of 1,1-Dimethyl-1,4-dihydrodibenzo[b,h][1,6]naphthyridinium iodides: turn-on type detection of DNA. *Eur J Org Chem* 2017: 6885–6888
13. Huang Q, Fu WL (2005) Comparative analysis of the DNA staining efficiencies of different fluorescent dyes in preparative agarose gel electrophoresis. *Clin Chem Lab Med* 43:841–842. <https://doi.org/10.1515/CCLM.2005.141>
14. Mahalakshmi G, Vennila KN, Selvakumar B, Rao PL, Malwade R, Deval S, Madhuri S, Seenivasaperumal M, Elango KP (2019) Spectroscopic investigations on DNA binding profile of two new naphthyridine carboxamides and their application as turn-on fluorescent DNA staining probes. *J Biomol Struct Dyn* 38:3443–3451. <https://doi.org/10.1080/07391102.2019.1657501>
15. Hu B, Deng L (2018) Catalytic asymmetric synthesis of trifluoromethylated  $\alpha$ -amino acids through the umpolung addition of trifluoromethyl imines to carboxylic acid derivatives. *Angew Chem Int Ed* 57:2233–2237. <https://doi.org/10.1002/ange.201710915>
16. Hyslop JF, Lovelock SL, Sutton PW, Brown KK, Allan WJB, Roiban GD (2018) Biocatalytic synthesis of chiral N-functionalized amino acids. *Angew Chem Int Ed* 57:13821–13824. <https://doi.org/10.1002/ange.201806893>
17. Hutchinson I, Jennings SA, Vishnuvajjala BR, Westwell AD, Stevens MFG (2002) Antitumor benzothiazoles. 16.<sup>1</sup> Synthesis and pharmaceutical properties of antitumor 2-(4-aminophenyl)benzothiazole amino acid prodrugs. *J Med Chem* 45:744–747. <https://doi.org/10.1021/jm011025r>
18. Odonovan MR, Mee CD, Fenner S, Teasdale A, Phillips DH (2011) Boronic acids—a novel class of bacterial mutagen. *Mutat Res* 724:1–6. <https://doi.org/10.1016/j.mrgentox.2011.05.006>
19. Yang W, Gao X, Wang B (2003) Boronic acid compounds as potential pharmaceutical agents. *Med Res Rev* 23:346–368. <https://doi.org/10.1002/med.10043>
20. Peng Q, Chen F, Zhong Z, Zhuo R (2010) Enhanced gene transfection capability of polyethylenimine by incorporating boronic acid groups. *Chem Commun* 46:5888–5890. <https://doi.org/10.1039/c0cc00877j>
21. Ling X, Zhong W, Huang Q, Ni K (2008) Spectroscopic studies on the interaction of pazufloxacin with calf thymus DNA. *J Photochem Photobiol B* 93:172–176. <https://doi.org/10.1016/j.jphotobiol.2008.07.008>
22. Gowda BG, Mallappa M, Shivakumar A, Nageshbabu R (2014) Spectrofluorimetric studies on the interaction of moxifloxacin with herring sperm DNA. *Int J Pharm Sci* 5:5276–5282. <https://doi.org/10.13040/IJPSR.0975-8232>
23. Jamshidvand A, Sahihi M, Mirkhani V, Moghadam M, Baltork IM, Tangestaninejad S, Rudbari HA, Kargar H, Keshavarzi R, Gharaghani S (2018) Studies on DNA binding properties of new Schiff base ligands using spectroscopic, electrochemical and computational methods: influence of substitutions on DNA-binding. *J Mol Liq* 253:61–71. <https://doi.org/10.1016/j.molliq.2018.01.029>
24. Ozkan S, Tok TT, Baran AU, Akbay N (2019) Multispectroscopic and computational investigation of CT-DNA binding properties with hydroxybenzylidene containing tetrahydrocarbazole derivative. *J Fluoresc* 29:101–110. <https://doi.org/10.1007/s10895-018-2314-4>
25. Shahabadi N, Shiri F, Hadidi S (2019) Studies on the interaction of antibiotic drug rifampin with DNA and influence of bivalent metal ions on binding affinity. *Spectrochim Acta A* 219:195–201. <https://doi.org/10.1016/j.saa.2019.04.059>
26. Niroomand S, Motlagh MK, Noroozifar M, Moodi A (2012) Spectroscopic studies on the binding of holmium-1,10-phenanthroline complex with DNA. *J Photochem Photobiol B* 117:132–139. <https://doi.org/10.1016/j.jphotobiol.2012.09.015>
27. Rad JA, Jarrahpour A, Aseman MD, Nabavizadeh M, Pourmejadi R, Heidari HR, Turos E (2019) Design, synthesis, DNA binding, cytotoxicity, and molecular docking studies of amonafide-linked  $\beta$ -lactam. *Chem Select* 4:2741–2746. <https://doi.org/10.1002/slct.201803785>
28. Bohlander PR, Wagenknecht HA (2013) Synthesis and evaluation of cyanine-styryldyes with enhanced photostability for fluorescent DNA staining. *Org Biomol Chem* 11:7458–7462. <https://doi.org/10.1039/c3ob41717d>
29. Bohlander PR, Wagenknecht HA (2015) Bright and photostable cyanine-styryl chromophores with green and red fluorescence colour for DNA staining. *Methods Appl Fluoresc* 3:044003. <https://doi.org/10.1088/2050-6120/3/4/044003>
30. Kaloyanova S, Trusova VM, Gorbenko GP, Deligiogiev T (2011) Synthesis and fluorescence characteristics of novel asymmetric cyanine dyes for DNA detection. *J Photochem Photobiol A* 217:147–156. <https://doi.org/10.1016/j.jphotochem.2010.10.002>
31. Bi S, Zhou H, Wu J, Sun X (2018) Micronomicin/tobramycin binding with DNA: fluorescence studies using of ethidium bromide as a probe and molecular docking analysis. *J Biomol Struct Dyn* 37: 1464–1476. <https://doi.org/10.1080/07391102.2018.1461138>
32. Wang L, Zhang G, Pan J, Xiong C, Gong D (2014) Intercalation binding of food antioxidant butylated hydroxanisole to calf thymus DNA. *J Photochem Photobiol B* 141:253–261. <https://doi.org/10.1016/j.jphotobiol.2014.10.011>
33. Silva CM, Silva MM, Reis FS, Ruiz ATG, Carvalho JE, Santos JCC, Figueiredo IM, Alves RB, Modolo LV, Fatima A (2017) Studies on free radical scavenging, cancer cell antiproliferation, and calf thymus DNA interaction of Schiff bases. *J Photochem Photobiol B* 172:129–138. <https://doi.org/10.1016/j.jphotobiol.2017.05.020>

34. Tian Z, Huang Y, Zhang Y, Song L, Qiao Y, Xu X, Wang C (2016) Spectroscopic and molecular modeling methods to study the interaction between naphthalimide-polyamine conjugates and DNA. *J Photochem Photobiol B* 158:1–15. <https://doi.org/10.1016/j.jphotobiol.2016.01.017>
35. Sarwar T, Rehman SU, Husain MA, Ishqi HM, Tabish M (2015) Interaction of coumarin with calf thymus DNA: deciphering the mode of binding by in vitro studies. *Int J Biol Macromol* 73:9–16. <https://doi.org/10.1016/j.ijbiomac.2014.10.017>
36. Husain MA, Ishqi HM, Rehman SU, Sarwar T, Afrin S, Rahman Y, Tabish M (2017) Elucidating the interaction of sulindac with calf thymus DNA: biophysical and in silico molecular modelling approach. *New J Chem* 41:14924–14935. <https://doi.org/10.1039/c7nj03698a>
37. Kumar A, Kumar A, Gupta RK, Paitandi RP, Singh KB, Trigun SK, Hundal MS, Pandey DS (2016) Cationic Ru(II), Rh(III) and Ir(III) complexes containing cyclic  $\pi$ -perimeter and 2-aminophenyl benzimidazole ligands: synthesis, molecular structure, DNA and protein binding, cytotoxicity and anticancer activity. *J Organomet Chem* 801:68–79. <https://doi.org/10.1016/j.jorganchem.2015.10.008>
38. Darabi F, Hadadzadeh H, Simpson J, Shahpiri A (2016) A water-soluble Pd(II) complex with a terpyridine ligand: experimental and molecular modeling studies of the interaction with DNA and BSA; and in vitro cytotoxicity investigations against five human cancer cell lines. *New J Chem* 40:9081–9097. <https://doi.org/10.1039/c6nj01880g>
39. Thomas RK, Sukumaran S, Sudarsanakumar C (2019) Photobehaviour and in vitro binding strategy of natural drug, chlorogenic acid with DNA: a case of groove binding. *J Mol Struct* 1178:62–72. <https://doi.org/10.1016/j.molstruc.2018.10.019>
40. Suganthi M, Elango KP (2016) Synthesis, characterization and serum albumin binding studies of vitamin K3 derivatives. *J Photochem Photobiol B* 166:126–135. <https://doi.org/10.1016/j.jphotobiol.2016.11.016>

**Publisher's Note** Springer Nature remains neutral with regard to jurisdictional claims in published maps and institutional affiliations.